https://doi.org/10.70882/kky1fj28

SCIENCE FORUM (JOURNAL OF PURE AND APPLIED SCIENCES) 26, (4) (2026), 1232 - 1249

Science Forum (Journal of Pure and Applied Sciences)

Journal Homepage: https://atbuscienceforum.com.ng/index.php/jpas

Computing the Wiener Index of Some Chemical Molecules from Shortest-Path Distance Matrices: A Pendant-Path Reduction Approach

Zeyad Mohammed Abed, Wisam Rafid Dawood

Department of Computer Sciences, College of Sciences, AL-Nahrain University, Jadriya, Baghdad, Iraq

Abstract

The Wiener index is one of the oldest distance-based graph invariants used in mathematical chemistry, obtained by summing the shortest-path distances between all unordered pairs of vertices of a connected graph. Throughout, molecules are represented by hydrogen-suppressed molecular graphs, and the matrices studied are shortest-path distance matrices of these graphs, not chemical reaction-pathway matrices. This paper surveys twenty recent open-access works (2021–2026) on the Wiener index of molecular graphs and formalizes a pendant-path reduction: a pendant path of k vertices is removed from a chemical tree, the distance matrix is recomputed on the smaller tree, and the contribution of the removed path is restored through a closed-form correction that depends only on k, the order n of the tree and the transmission of the anchor vertex in the reduced tree. For a representative ten-vertex tree, removing a pendant path of three vertices reduces the number of independent distance entries from 45 to 21 (about 53%) while exactly reproducing $W(G) = 158$. A MATLAB implementation computes the Wiener index of nineteen molecular graphs (the reference tree, the n-alkanes C_1–C_{10}, the cycles C_3–C_8, and the dendrimers $T_{2,3}$ and $T_{3,3}$); the direct, leaf-deletion and pendant-path computations agree wherever applicable, and the values match known closed-form expressions. At these small sizes the reduction gives no wall-clock speedup, and its benefit is analytic. The proposed reduction is shown to be the multi-vertex generalisation of the linear-time leaf-deletion algorithm and a closed-form simplification of the cut method for pendant paths.

Keywords

Wiener index,
Shortest-path distance matrix,
Chemical graph,
Graph reduction,
Molecular graph,
Topological index,
Alkanes,
Dendrimers.

EISSN: 3156-5190 (Online)
ISSN: 1119-4618 (Print)
JPAS
Faculty of Science, ATBU Bauchi

Corresponding Author: Zeyad Mohammed Abed, Department of Computer Sciences, College of Sciences, AL-Nahrain University, Jadriya, Baghdad, Iraq. Email: zeyad.mohammed@nahrainuniv.edu.iq © 2026 Faculty of Science, ATBU Bauchi. All rights reserved

1. Introduction

1.1. Motivation. The Wiener index is the oldest distance-based graph index used in mathematical chemistry [5, 2, 7, 16]. Presented by Harry Wiener in 1947 in the study of the boiling points of alkanes [2, 16, 15, 14], it is given by the sum of distances among all unordered pairs of vertices in a connected graph and has since been used to estimate many physico-chemical properties, including key constants, density, viscosity, surface tension, and ultrasonic sound velocity [2]. Bi et al. describe the Wiener index as one of the oldest and most widely used graph indices [2], and Vaidya and Li note that vulnerability measures and graph indices are central to problems such as the stability of communication networks and the construction of mathematical models for chemical compounds [17].

The molecular graph of a molecule is a connected graph in which each non-hydrogen atom is represented by a vertex and each chemical bond by an edge [5]. The Wiener index of such a graph encodes information about the size and branching of the molecule, and thereby about macroscopic properties that depend on the underlying structure. Damnjanović, Xu, and Xu define a molecular graph as one whose maximum degree is at most four, since any carbon atom in organic compounds forms four chemical bonds [5], and Tabassum et al. note that dendrimers are highly branched organic macromolecules built from repeated iterations of branched units [16]. The Wiener index is well defined on any such structure, from the linear alkane skeleton P_n and the cyclic six-membered skeleton C_6 to the highly branched dendrimer $T_{r,\delta}$ and the spherical fullerene C_{60}.

1.2. Problem statement. The standard method for computing the Wiener index of a molecular graph begins with the construction of the $n \times n$ distance matrix $D(G)$, whose entry d_{uv} records the length of a shortest path between vertices u and v. Brezovnik, Tratnik, and Žigert Pleteršek state that this construction proceeds by the well-known Floyd-Warshall method [4], whose cost is $O(n^3)$ in the number of atoms n. Once $D(G)$ is available, the Wiener index is recovered by summing the entries above the diagonal at an additional cost of $O(n^2)$. For short molecules the cubic cost is not a concern, but for large dendrimers, nanosheets, or fullerene oligomers the matrix grows quickly: Sabirov et al. report Wiener-index values in excess of 10^6 for the $(C_{60})_6$ oligomer [14], whose 360×360 distance matrix has about 1.3×10^5 entries, $64\,620$ of them independent.

Bi et al. [2] address this problem through a linear-time method for acyclic and unicyclic graphs, in which each leaf vertex is removed in turn and the edge it drops contributes $\mathrm{count}[v] \cdot (n - \mathrm{count}[v])$ to the running Wiener-index total. Klavžar and Romih [10] generalise the same idea through the cut method on hypergraphs: edges are partitioned into Θ-classes and the Wiener index is recovered from the products of component sizes after each class is removed. Dankelmann [6] phrases the same principle at the level of the distance sequence, showing that vertex deletion is the basic step in bounding any distance-based descriptor in a unified way. The common element among these works is that the size of the molecular graph can be reduced before the Wiener index is computed, with the contribution of the removed structure recovered through a closed-form expression that depends on the size of that structure rather than on a fresh distance computation.

In this study we formalise a fixed instance of this cut. A tree of ten vertices is treated as a representative molecular graph; a pendant path of three vertices is removed; the distances among the remaining seven vertices are kept unchanged, and the missing contribution is recovered by adding a correction that depends on the number of removed vertices and on the transmission of the vertex to which the path was attached. The challenge is to verify that this cut reproduces the Wiener index of the original graph, to identify the closed-form correction, and to check the method on a range of molecular graphs that appear in recent work.

Terminology. Throughout the paper, a *path* is a graph-theoretic path in the molecular graph, and the distance matrix $D(G)$ is the matrix of shortest-path lengths, that is, the numbers of bonds on a shortest bond path between pairs of non-hydrogen atoms. The matrices computed here are therefore shortest-path distance matrices; no chemical reaction pathway, reaction coordinate, or reaction network is

modelled, and the results do not describe how one molecule is transformed into another.

1.3. Aim and contributions. This work has three main objectives. The first is to survey twenty recent works (2021–2026) on the Wiener index and on related distance-matrix and cut techniques, identifying for each its contribution to the matrix-based computation of the Wiener index on molecular graphs. The second is to formalise the pendant-path cut by finding the precise closed-form contribution that the removed path makes to the Wiener index, expressed in terms of the number of removed vertices and the transmission of the anchor vertex in the reduced graph. The third is to implement the cut in MATLAB, apply it to the ten-vertex tree and to three further molecular families (n-alkanes from C_1 to C_{10}, cycles from C_3 to C_8, and the dendrimers $T_{2,3}$ and $T_{3,3}$), and verify that the Wiener-index values found by the cut agree, wherever the methods are applicable, with those found by direct Floyd-Warshall summation and by the linear-time leaf-deletion method of Bi et al. [2].

The contributions are thus both expository and computational. On the expository side, the work organises the contributions of twenty references into a single classification scheme, grouped by category (core theory, distance matrix and cut, trees and paths, chemical applications, variants), and identifies the closest published precursors for each part of the cut. On the computational side, the work documents Wiener-index values for nineteen molecular graphs on a uniform code base, reports that at these sizes the reduction yields no wall-clock speedup over direct summation, so that its benefit is analytic rather than computational, and confirms that the computed values reproduce the closed-form expressions $W(P_n) = n(n^2-1)/6$ for paths and $W(C_n) = n^3/8$ for even cycles, the dendrimer values of $T_{2,3}$ and $T_{3,3}$ obtained independently from the edge decomposition and from the path counts of Tabassum et al. [16], and the chemical-tree results of Damnjanović et al. [5].

Figure 1 illustrates the relationship among a short molecule (propane), its hydrogen-suppressed graph $G = P_3$, and the corresponding 3×3 distance matrix $D(G)$; the Wiener index $W(G)$ of propane is the sum of the upper-triangular entries of $D(G)$, giving $W(P_3) = 4$.

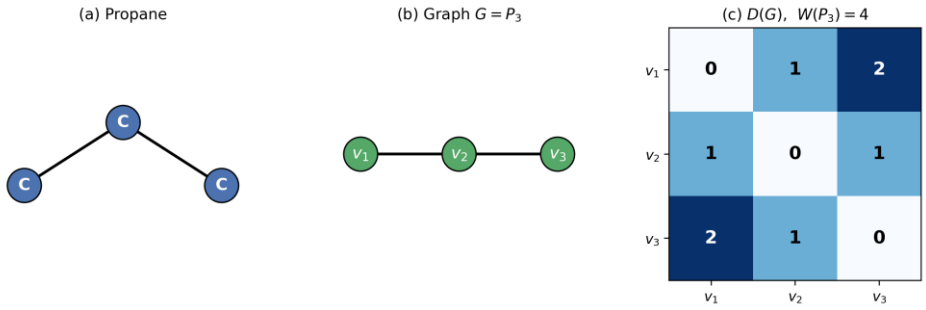


Figure 1. The relationship among propane, its hydrogen-suppressed graph $G = P_3$, and the corresponding 3×3 distance matrix $D(G)$. The Wiener index $W(P_3) = 4$ is the sum of the upper-triangular entries of $D(G)$.

1.4. Organisation. The remainder of the work is organised as follows. Section 2 collects the graph-theoretic and chemical-graph definitions used throughout, the distance matrix and the transmission, the Wiener index and its main variants, and the Hosoya polynomial that connects them. Section 3 documents the review methodology used to assemble the twenty references. Section 4 states the pendant-path cut and traces it to its closest published precursors. Section 5 organises the contributions of the twenty references into a single classification scheme. Section 6 reports the numerical results found by the MATLAB code. Section 7 notes the cost-benefit profile of the cut and its limitations. Section 8 concludes.

2. Background and Preliminaries

This section collects the definitions and notation used throughout the work. Each concept is drawn from the surveyed references and stated in the terminology used there.

2.1. Graphs and molecular graphs. A simple connected graph $G = (V, E)$ consists of a finite non-empty vertex set $V(G) = \{v_1, v_2, \dots, v_n\}$ and an edge set $E(G)$ of unordered pairs of distinct vertices. The order of G is $n = |V(G)|$ and the size of G is $m = |E(G)|$. A tree is a connected acyclic graph; a tree on n vertices has exactly $n - 1$ edges. A path P_n on n vertices has vertex set $\{v_1, \dots, v_n\}$ and edges $\{v_i v_{i+1} : 1 \le i \le n-1\}$. A cycle C_n on n vertices is obtained from P_n by adding the edge $v_n v_1$.

A connected graph whose maximum degree is at most four is called a molecular graph, because each non-hydrogen atom in an organic compound forms at most four chemical bonds [5]. Damnjanović, Xu, and Xu state that a molecular graph represents a chemical molecule in mathematical chemistry because any carbon atom in organic compounds forms four chemical bonds [5]. The hydrogen-suppressed graph of an n-alkane is the path graph P_n on its n carbon atoms; the corresponding graph of cyclohexane is the cycle C_6.

Chemical interpretation. All graphs in this paper are hydrogen-suppressed connectivity models: vertices are non-hydrogen atoms, edges are bonds, and bond multiplicity, atom type, charge, stereochemistry and three-dimensional geometry are not encoded. Consequently, two molecules with the same graph topology have the same distance matrix and the same Wiener index even when their chemical properties differ. For example, the cycle C_6 is the hydrogen-suppressed graph of both cyclohexane and benzene and gives $W(C_6) = 27$ for both, although one is a saturated and the other an aromatic compound; similarly, methane reduces to a single vertex with $W = 0$. Wiener-index values are therefore used here as topological descriptors, and any link to physico-chemical properties must be established through separate structure–property models [2, 14]. Bond multiplicities can be included through the weighted Wiener index of Brezovnik et al. [4], which is outside the present scope.

A dendrimer $T_{r,\delta}$ is defined as the rooted tree of radius r in which every vertex at distance less than r from the root has degree δ [16]; it is denoted $T_{n,k}$ in [16], and the symbols r and δ are used here to avoid a clash with the order n and the path length k of Section 4. The dendrimer $T_{2,3}$ therefore has a root of degree three, three internal vertices each of degree three, and six leaves, for a total of ten vertices, and $T_{3,3}$ has $1 + 3 + 6 + 12 = 22$ vertices. Tabassum et al. note that dendrimers are highly branched organic macromolecules built from repeated iterations of branched units and are used in a variety of fields including chemistry, nanotechnology, and biology [16].

2.2. The distance matrix and the transmission. The distance $d_G(u, v)$ between two vertices u and v of a connected graph G is the number of edges on a shortest path between them. The all-pairs distances form the $n \times n$ distance matrix $D(G) = (d_{uv})$, which is symmetric, has a zero diagonal, and obeys the triangle inequality [9]. The distance matrix is the principal data structure from which every distance-based graph index is computed [4, 15, 11].

The transmission of a vertex v in G is the sum of distances from v to all other vertices,

$$\mathrm{Tr}_G(v) = \sum_{u \in V(G)} d_G(u, v),$$

and v is called transmission-regular if $\mathrm{Tr}_G(v)$ is the same for every vertex of G [9, 8]. The distance Laplacian matrix of G is defined as

$$D^L(G) = \mathrm{Tr}(G) - D(G),$$

where $\mathrm{Tr}(G)$ is the diagonal matrix of vertex transmissions [9, 11]. The matrix $D^L(G)$ is real, symmetric, and positive semi-definite, with smallest eigenvalue zero.

2.3. The Wiener index. The Wiener index $W(G)$ of a connected graph G is the sum of all pairwise distances between unordered pairs of vertices,

$$W(G) = \sum_{\{u,v\} \subseteq V(G)} d_G(u, v),$$

a definition that is uniform among the surveyed works [10, 7, 4, 8, 19, 18]. An equivalent expression in terms of vertex transmissions, used by Ibrahim et al. [8] and by Khan and Pirzada [9], is

$$W(G) = 1/2 \sum_{v \in V(G)} \mathrm{Tr}_G(v).$$

For trees, Abu-Affash et al. [1] state the edge-decomposition formula

$$W(T) = \sum_{(p,q)\in E(T)} N_T(p) \cdot N_T(q) \cdot |pq|, \tag{5}$$

where $N_T(p)$ and $N_T(q)$ denote the numbers of vertices on the two sides of the edge (p, q) after it is removed, and $|pq|$ is the edge length (equal to 1 for an unweighted graph). The same decomposition underlies the linear-time leaf-deletion method of Bi et al. [2], in which each leaf vertex is removed in turn and the edge it drops contributes $\mathrm{count}[v] \cdot (n - \mathrm{count}[v])$ to the running total, where $\mathrm{count}[v]$ is the number of vertices already removed in the subtree behind v.

The Wiener index was introduced by Harry Wiener in 1947 in the study of the boiling points of alkanes [2, 16, 15, 14]. Vaidya and Li note that in 1947 Harry Wiener introduced a graph index linked to molecular branching [17], and Brezovnik et al. state that the distance-based definition on graphs was first given by Hosoya [4].

2.4. Variants of the Wiener index. Several variants of the Wiener index have been introduced to capture specific chemical or combinatorial properties. The hyper-Wiener index is $WW(G) = \frac{1}{2}\sum[d(u,v) + d(u,v)^2]$ and was introduced by Randić [13, 6, 19, 15]. The Harary index $H(G) = \sum 1/d(u,v)$ rewards short pairwise distances [6, 17, 19]. The Tratch–Stankevitch–Zefirov index is $TSZ(G) = \frac{1}{6}Q'''(1)$, where $Q(x) = x^2 H(G,x)$ and $H(G,x)$ is the Hosoya polynomial of Section 2.5 [17, 15]. The peripheral Wiener index restricts the pairwise sum to peripheral vertices, and its hyper analogue $PWW(G)$ was introduced by Rabenantoandro [13]. The Steiner k-Wiener index $SW_k(G)$ extends the pairwise distance to the Steiner distance of k-vertex subsets and coincides with the Wiener index when $k = 2$ [18]; here k is the subset size, used only in this definition. The generalised Wiener index $W_g(G) = \sum g\big(d_G(s,t)\big)$ recovers the Wiener, hyper-Wiener, Harary, and modified Wiener indices as special cases [19]. The Kirchhoff index $Kf(G)$ is the sum of resistance distances and is closely related to the Laplacian spectrum [20]. The Gutman index $Gut(G) = \sum \deg(u)\deg(v)\, d(u,v)$ weights each pairwise distance by the product of the endpoint degrees [12]. The weighted Wiener index W_a, introduced by Brezovnik et al., extends the distance to edge-weighted graphs to model multiple chemical bonds [4].

Table 1 lists the principal variants of the Wiener index encountered in the surveyed references, together with their defining formula and a representative reference. Figure 2 organises the same variants in a hierarchical taxonomy that radiates from the classical $W(G)$ at the top; the references attached to each variant are those of Table 1.

Table 1. Principal variants of the Wiener index encountered in the surveyed references.

Variant	Definition	Reference
Wiener index $W(G)$	$\sum d(u,v)$	[10, 2, 7, 4]
Hyper-Wiener $WW(G)$	$1/2\sum[d + d^2]$	[13, 6, 15]
Peripheral hyper-Wiener $PWW(G)$	$1/2\sum_{\mathrm{Peri}}[d + d^2]$	[13]
Steiner k-Wiener $SW_k(G)$	$\sum d_G(S)$	[18]
Wiener–Hosoya matrix $WH(G)$	$w_{ij} = \sigma_i/(2d_i) + \sigma_j/(2d_j)$	[8]
Weighted Wiener $W_a(G^D)$	edge-weighted W	[4]
Generalised Wiener $W_g(G)$	$\sum g\big(d(s,t)\big)$	[19]
Harary $H(G)$	$\sum 1/d(u,v)$	[6, 17, 19]
Kirchhoff $Kf(G)$	$\sum$ resistance distances	[20]
Gutman $Gut(G)$	$\sum d(u)d(v)d(u,v)$	[12]
Distance Laplacian $D^L(G)$	$\mathrm{Tr}(G) - D(G)$	[9, 11]
Hosoya polynomial $H(G,x)$	$\sum p(G,d)\, x^d$	[17, 8, 15]
TSZ index	$\frac{1}{6}Q'''(1),\ Q = x^2 H$	[17, 15]

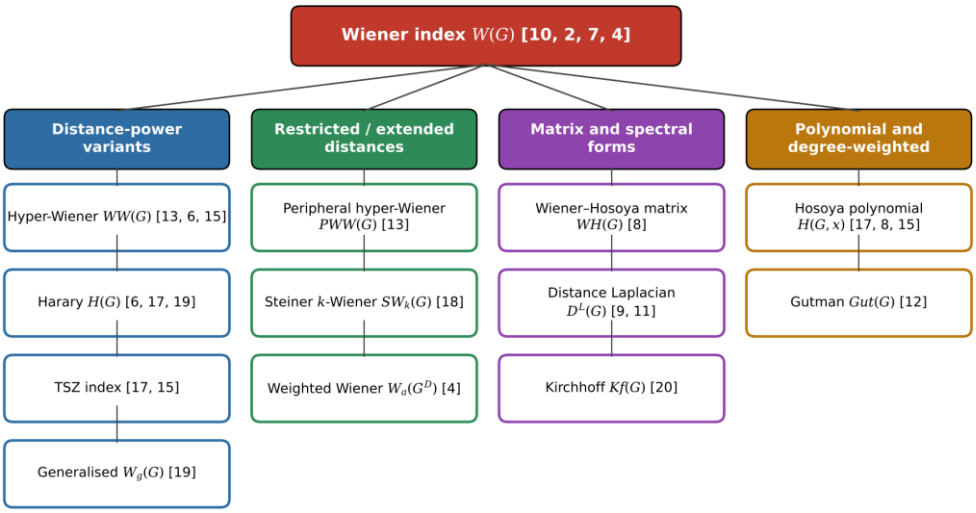


Figure 2. Taxonomy of the Wiener-index variants listed in Table 1, grouped into four families; the bracketed numbers are the references given for each variant in Table 1.

The Wiener-index variants most relevant to this study are $W(G)$ itself and the Wiener–Hosoya matrix $WH(G)$ of Ibrahim et al. [8]: an $n \times n$ matrix with off-diagonal entries $w_{ij} = \sigma_i/(2d_i) + \sigma_j/(2d_j)$ on edges $(i,j) \in E(G)$ and zero elsewhere, where σ_i is the transmission of vertex i and d_i its degree. Ibrahim et al. prove that one half of the sum of all entries of $WH(G)$ equals the Wiener index of G, giving another way to compute it [8].

2.5. The Hosoya polynomial. The Hosoya polynomial of a graph G is the generating function

$$H(G,x) = \sum_{d=1}^{\operatorname{diam}(G)} p\,(G,d) \cdot x^d, \tag{6}$$

where $p(G,d)$ is the number of unordered pairs of vertices at distance d and $\operatorname{diam}(G)$ is the diameter of G [17, 15]. Vaidya and Li show that the Wiener index is the first derivative of the Hosoya polynomial evaluated at $x = 1$, that is $W(G) = H'(G,1)$, and that the hyper-Wiener, TSZ, and Harary indices can be similarly obtained as derivatives or integrals of the Hosoya polynomial [17]. Sheikh et al. apply the Hosoya polynomial to compute the Wiener, hyper-Wiener, and TSZ indices of the $C_4C_8(R)$ and $C_4C_8(S)$ nanosheets [15].

The Hosoya polynomial and the distance matrix are complementary encodings of the same pairwise-distance information: the polynomial records the frequency of each distance value, while the matrix records the location of each distance entry in the graph. The reduction proposed here operates on the distance matrix and therefore preserves the information needed to recompute any descriptor that depends only on pairwise distances.

3. Review Methodology

This section documents how the twenty references that anchor the present work were selected, in line with reproducibility standards adopted in systematic literature reviews on topological indices.

3.1. PICOC framework. The scope of the review was framed by the PICOC structure, adapted from systematic-review practice to the present mathematical-chemistry setting. The *population* consists of chemical, molecular, and combinatorial graphs on which the Wiener index is defined. The *intervention* is any method that computes, bounds, characterises, or reduces the Wiener index $W(G)$ or a closely related variant. The *comparison* is a cross-comparison among methods (cut method, leaf-deletion, distance-matrix construction, closed-form formulas, spectral approaches). The *outcome* is a documented numerical value of $W(G)$, a closed-form expression, an algorithm with stated complexity, or an extremal characterisation. The *context* is published, open-access, peer-reviewed or arXiv-preprint sources between 2021 and 2026.

3.2. Search query and databases. The search was conducted on arXiv.org (with the queries "Wiener index chemical graph", "Wiener index

distance matrix", "Wiener index trees", and "Wiener index molecules alkanes") and on the MDPI journals *Mathematics*, *Symmetry*, and *Axioms* (with the query "Wiener index"). Each query was restricted to 2021–2026 and to open-access sources. The combined initial pool contained 44 candidate papers (27 from arXiv, 17 from MDPI), filtered to 20 papers using the inclusion and exclusion criteria of Table 2.

Table 2. Inclusion and exclusion criteria used to filter the twenty references from the 44-paper candidate pool.

Criterion	Inclusion	Exclusion
Publication year	2021–2026	Outside the window
Access	Open access, full PDF	Behind paywall
Language	English	Other languages
Format	Peer-reviewed journal or arXiv preprint	Conference abstracts only, slides, blog posts
Topic centrality	Wiener index or close variant is the principal object	Wiener index mentioned only in passing
Mathematical content	Explicit definition, formula, theorem, or algorithm involving W	Purely qualitative discussion
PDF integrity	Valid PDF (≥ 6 pages, ≥ 80 KB)	Corrupted or stub files
Relevance to the 8 axes	Covers at least 3 of the 8 axes	Covers fewer than 3

3.3. Snowballing. After the initial keyword-driven search, one round of backward snowballing was performed: the reference lists of the ten highest-relevance papers were scanned for further candidates within the 2021–2026 window. Three candidates were identified in this way (a Steiner-Wiener paper, a Hosoya-polynomial paper, and a distance-Laplacian paper); all three were already in the original pool, so snowballing did not enlarge the candidate set. No forward snowballing was performed.

3.4. Quality assessment and data extraction. Each candidate was scored against five criteria adapted from standard SLR practice: a clear Wiener-index definition, a clear procedure, a stated main result, stated limitations or future work, and open access. The scoring is reported in Table 7 of Section 7; all twenty retained references scored at least $4/5$. For each retained reference a ten-point structured summary was produced, recording bibliographic information, the problem studied, the procedure, coverage of the eight thematic axes, datasets and molecules, main formulas, numerical results and theorems, stated limitations, stated future work, and quotable phrases. All quotations were checked against the source PDFs at the page level. The search strings are listed in Section 3.2; the catalogue of the twenty references with their axis coding (Table 4) and quality scores (Table 7) is provided in Supplementary File S3, and the screening log of the 44 candidates is available from the corresponding author on reasonable request.

4. Methodology — Proposed Reduction Approach

This section states the path-removal cut and links it to established work. The construction has three layers: the standard matrix-based computation of the Wiener index, a direct summation form, and the cut that removes a leaf path from the molecular graph before recomputing the distances. A worked example on the ten-vertex tree closes the section.

4.1. Building the distance matrix. For a connected graph G with vertex set $V(G) = \{v_1, \dots, v_n\}$, the distance matrix is the $n \times n$ matrix $D(G) = (d_{uv})$

whose entry d_{uv} equals the length of a shortest path between u and v [9]. The matrix is symmetric with zero diagonal and satisfies the triangle inequality. To compute $D(G)$ from the adjacency matrix of a molecular graph, the Floyd–Warshall method is the standard tool [4]. Brezovnik et al. state explicitly that they use the well-known Floyd–Warshall method to compute the distance matrix D of (G, w) [4]. The method iterates over each triple of vertices and updates each entry in $O(n^3)$ time. The same $n \times n$ form underlies the Wiener–Hosoya matrix of Ibrahim et al. [8], the distance Laplacian matrix of Khan and Pirzada [9], and the distance-matrix construction of Sheikh et al. for the C_4C_8 nanosheets [15].

4.2. Direct Wiener-index computation. Once the distance matrix is available, the Wiener index of G is the sum of distances over all unordered pairs of vertices, as in (3), the definition used uniformly among the surveyed works [4]. The equivalent vertex-transmission form (4) is used by Ibrahim et al. and by Khan and Pirzada [9, 8], and for trees the edge-decomposition formula (5) is recorded by Abu-Affash et al. [1]. Computed directly from $D(G)$ by summation over the upper triangle, the cost of finding $W(G)$ is $O(n^2)$, dominated by the $O(n^3)$ cost of building $D(G)$.

4.3. Reduction by path removal. The central observation is that, for a chemical tree, the size of the distance matrix can be reduced before the Wiener index is computed. The same principle has been formalised in three closely related forms. The cut method of Klavžar and Romih partitions the edges of a graph into Θ-classes; once a class is removed, the graph breaks into components, and the Wiener index is recovered from the products of component sizes [10]. Klavžar and Romih describe the underlying idea as first partitioning the edges of a molecular graph and then, by deleting parts of the partition, building smaller weighted quotient graphs [10]. A second formulation, due to Bi et al., is the leaf-deletion linear-time algorithm in which each pendant vertex is removed in turn and its contribution accumulated by the rule that a total of $\mathrm{count}[v] \cdot (n - \mathrm{count}[v])$ shortest paths pass through the dropped edge [2]. A third formulation is the vertex-removal inequality of Dankelmann, expressed at the level of the distance sequence [6].

The path-removal cut sits inside this family. Let T be a tree of order n and let $P = u_1u_2 \cdots u_k$ be a pendant path of $k \geq 1$ vertices attached to a vertex a of T by the edge au_1, where $\deg(u_i) = 2$ for $1 \leq i \leq k-1$ and $\deg(u_k) = 1$. Throughout, k counts the removed *vertices*; their removal deletes the k edges $au_1, u_1u_2, \ldots, u_{k-1}u_k$, that is, the $k-1$ edges of P together with the attaching edge. The vertex a is called the *anchor*, and $T' = T - \{u_1, \ldots, u_k\}$ is the reduced tree of order $n-k$, with a distance matrix $D(T')$ of order $(n-k) \times (n-k)$. Distances inside T' are unchanged, because no shortest path between two vertices of T' passes through P. The distances from the removed vertices are not computed from scratch but restored in closed form, in the same spirit as the edge-contribution formula of Bi et al. [2] and the path-replacement transformations of Damnjanović et al. [5]. The recursive structure of dendrimers studied by Tabassum et al. gives a complementary view, in which $T_{r,\delta}$ is built from $T_{r-1,\delta}$ by attaching pendant branches [16].

The closed-form correction restoring the contribution of the removed pendant path of k vertices is

$$W_{\text{path}} = W(P_k) + (n-k) \cdot \frac{k(k+1)}{2} + k \cdot \mathrm{Tr}_{T'}(\text{anchor}), \qquad (7)$$

where a (the *anchor*) is the vertex of the reduced tree T' adjacent to the removed path, and $Tr_{T'}(a)$ is its transmission in T', defined by (1). The full Wiener index is then recovered as $W(T) = W(T') + W_{path}$. To verify (7), note that $d(u_i, a) = i$ and that every path from u_i to a vertex v of T' passes through a, so $d(u_i, v) = i + d_{T'}(a, v)$. The pairs of vertices of T fall into three classes: pairs inside T', contributing $W(T')$; pairs inside P, contributing $\sum_{1 \leq i < j \leq k} (j-i) = W(P_k) = k(k^2-1)/6$; and mixed pairs, contributing $\sum_{i=1}^{k} \sum_{v \in V(T')} \big(i + d_{T'}(a, v)\big) = (n-k)\frac{k(k+1)}{2} + k\, Tr_{T'}(a)$, since $|V(T')| = n-k$ and $d_{T'}(a, a) = 0$. The last two classes together give (7).

4.4. The ten-vertex example. The example is a tree of ten vertices from which a pendant path of $k = 3$ vertices is removed. The full distance matrix of the original tree has one hundred entries, of which forty-five are independent (the matrix is symmetric with zero diagonal). After the three path vertices are removed, the reduced tree has seven

vertices and its distance matrix has only twenty-one independent entries. The distances among the seven remaining vertices are unchanged, because the removed vertices lie on a pendant path and do not appear on any shortest path between two remaining vertices, a fact that also underlies the leaf-deletion analysis of Bi et al. [2]. The contribution of the removed path to $W(G)$ is obtained through (7); the complete numerical derivation is given in Section 6.3. Figure 3 shows the tree together with the before-and-after distance matrices, and Table 3 summarises the three computation modes used in the work.

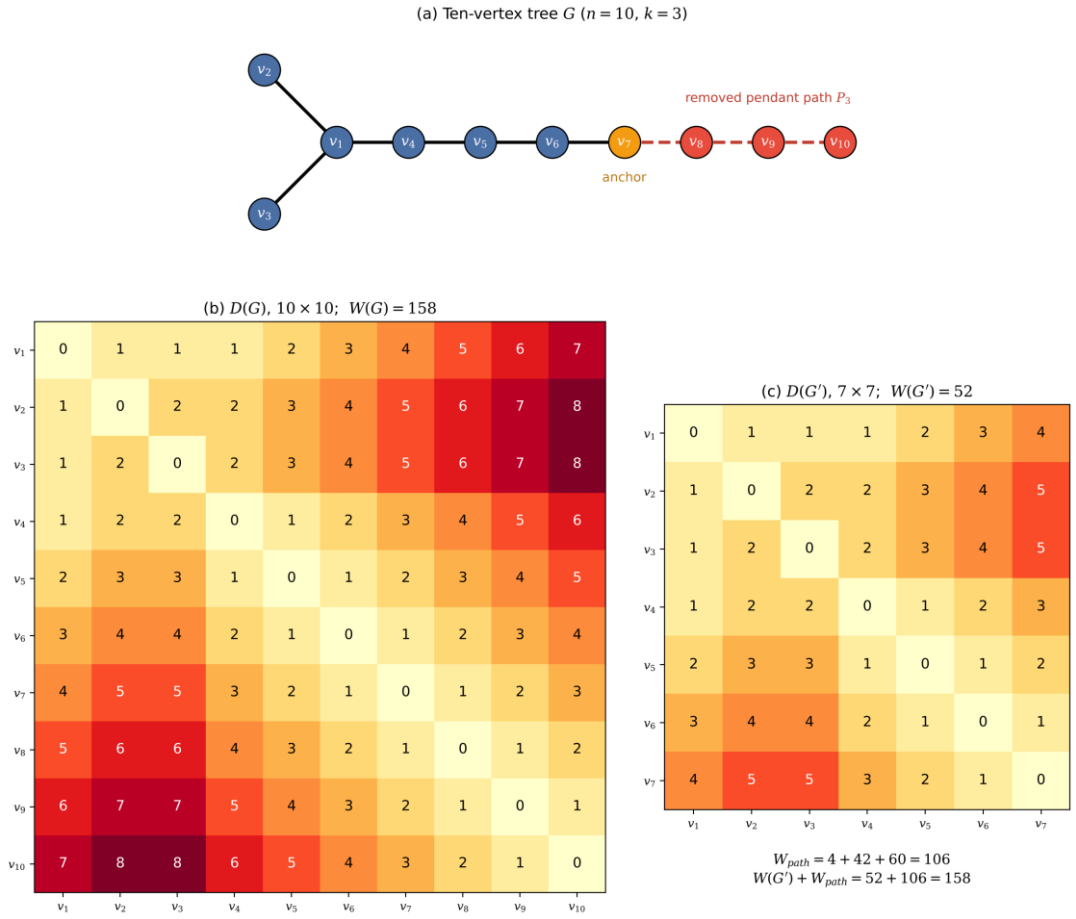


Figure 3. The ten-vertex reference tree under the proposed cut: (a) the tree G (edge list in Section 6.3), with anchor v_7 and removed pendant path $v_8v_9v_{10}$; (b) the 10×10 distance matrix $D(G)$; (c) the 7×7 distance matrix $D(G')$ of the reduced tree.

Table 3. Three modes of Wiener-index computation evaluated in Section 6.

Mode	Description	Complexity	Source
Floyd–Warshall + sum	Build $n \times n$ distance matrix $D(G)$, sum upper triangle	$O(n^3) + O(n^2)$	[4]
Edge-contribution (leaf-deletion)	Iteratively remove pendant vertices; accumulate $\text{count}[v] \cdot (n - \text{count}[v])$	$O(n)$	[2]
Pendant-path reduction (proposed)	Remove pendant path of k vertices; $W = W(T') + W_{\text{path}}$	$O((n-k)^3) + O(n)$	This paper

4.5. Implementation outline. The code, written in MATLAB, proceeds in five stages. First, the adjacency matrix of the molecular graph is built from the atom–bond list of the molecule, following the molecular-graph construction of Brezovnik et al. [4] and Sheikh et al. [15]. Second, the Floyd–Warshall method computes the full distance matrix $D(G)$ [4]. Third, the Wiener index $W(G)$ is found by direct summation over the upper triangle of $D(G)$. Fourth, the cut of Section 4.3 is applied: a leaf path of length k is detected, its k vertices are removed, the new distance matrix $D(G')$ is computed on the smaller graph, and the contribution of the removed path is added back through (7). Fifth, the running times of the full and reduced computations are recorded for each test molecule.

5. Comparative Analysis

The twenty references span five overlapping categories: core Wiener-index theory, distance-matrix and reduction techniques, tree- and path-focused investigations, chemical and molecular applications, and Wiener-index variants. Table 4 condenses the coverage of the twenty references across eight thematic axes, and Figure 4 shows the distribution of computational-technique families.

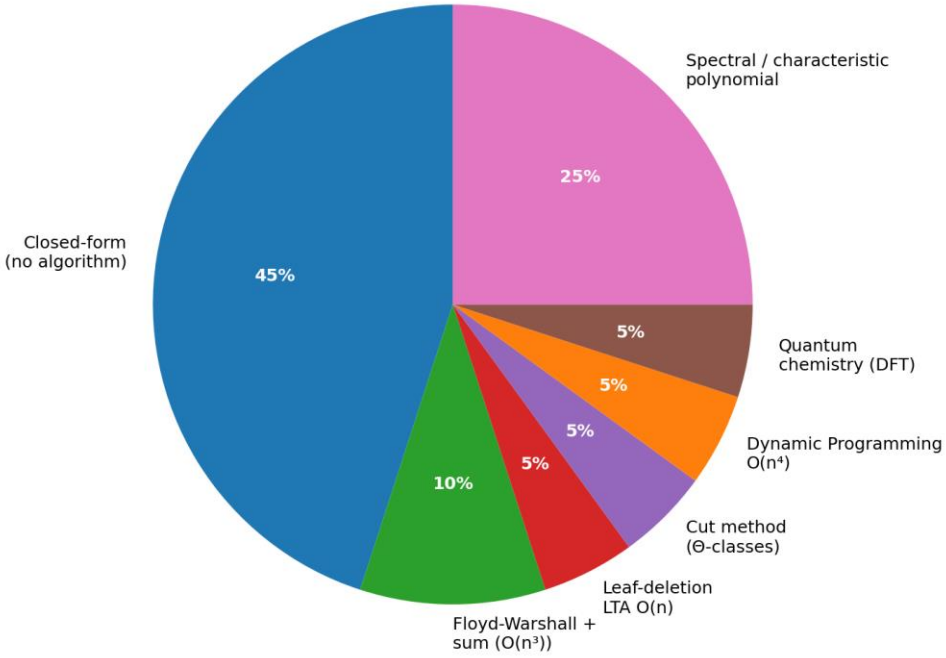


Figure 4. Computational-technique families used by the twenty surveyed references.

Table 4. Master comparison matrix: twenty references versus eight thematic axes. An entry is • if the axis is explicitly addressed by the reference, and blank otherwise; the last row gives the number of references marked on each axis.

Ref	W theory	D-matrix	Reduction	Trees/paths	Chem. mol.	Comp. algo	Variants	Hosoya
[5]	•		•	•	•	•	•	
[3]	•		•	•				
[13]	•		•	•			•	
[10]	•		•	•	•	•		
[1]	•		•	•		•		
[2]	•	•	•	•	•	•	•	
[7]	•		•	•			•	•
[6]	•		•	•	•		•	•
[9]	•	•	•				•	
[17]	•			•	•		•	•
[16]	•		•	•	•			•
[4]	•	•		•	•	•	•	•
[8]	•	•			•		•	•
[19]	•		•		•		•	
[18]	•		•	•			•	
[20]	•			•	•		•	
[15]	•	•			•	•	•	•
[14]	•	•			•	•	•	
[11]	•	•		•			•	
[12]	•		•	•	•		•	
Σ	**20**	**7**	**13**	**15**	**13**	**7**	**16**	**7**

5.1. Distance-matrix-based works. Seven of the twenty references build an explicit distance-related matrix and treat it as the principal object of study. Khan and Pirzada [9] introduce the distance Laplacian matrix $D^L(G) = \mathrm{Tr}(G) - D(G)$ and obtain bounds on its spread in terms of the Wiener index and the maximum transmission degree. Li and Zhou [11] follow the same matrix framework for the distance Laplacian energy of unicyclic and bicyclic graphs. Ibrahim et al. [8], Brezovnik et al. [4], Sheikh et al. [15], and Sabirov et al. [14] likewise take the distance matrix or a weighted variant as the starting point of the Wiener-index computation.

5.2. Reduction techniques in the literature. Thirteen references use some form of graph reduction. The cut method of Klavžar and Romih [10], the leaf-deletion algorithm of Bi et al. [2], and the distance-sequence majorisation of Dankelmann [6] are the three closest precursors of the pendant-path cut. The extremal-tree transformations of Damnjanović et al. [5] and Borovićanin et al. [3] reduce trees by relocating pendant paths, and the recursive dendrimer construction of Tabassum et al. [16] reduces $T_{r,\delta}$ to $T_{r-1,\delta}$.

5.3. Chemical molecules covered in the literature. Thirteen references treat explicit chemical molecules or molecular graph families: alkanes and alkadienes [4], dendrimers [16], nanosheets [15], fullerene oligomers [14], and tetrahedrane-derived compounds [20], among others. These molecules form the basis of the test set used in Section 6.

6. RESULTS

This section reports the numerical results produced by the MATLAB implementation of Section 4. Three computation modes were evaluated on every test molecule to which they apply: the full Floyd-Warshall construction followed by direct summation, the linear-time leaf-deletion procedure of Bi et al. [2] for trees, and the proposed pendant-path reduction.

6.1. Test set and experimental setup. Five families of molecular graphs were studied. The ten-vertex tree was used as the reference case for the cut. The n-alkane series C_1 to C_{10} was modelled as the path graph P_n, following the convention of Brezovnik et al. [4]. Cycle graphs C_3 to C_8 were included as hydrogen-suppressed models of cycloalkane and benzenoid-type rings in the spirit of Sheikh et al. [15] and Mei and Miao [12]. Two dendrimers, $T_{2,3}$ and $T_{3,3}$, were built from the recursive definition of Tabassum et al. [16]. The complete test set thus covered nineteen molecular graphs spanning trees, linear series, cycles, and highly branched structures. Not every mode applies to every family. The direct Floyd–Warshall computation applies to all nineteen graphs. Leaf-deletion [2] and the pendant-path reduction require a pendant vertex; they were applied to the reference tree (with $k = 3$), to the alkanes C_2–C_{10}, and to the two dendrimers (where the longest pendant path has $k = 1$), whereas C_1 is a single vertex with $W = 0$ and the cycles C_3–C_8 have no pendant vertex (Section 7.3). The modes used for each graph are listed in Table 5. All computations were carried out in MATLAB [release] on a single workstation ([processor, memory, operating system]); the timing protocol is described in Section 6.4.

6.2. Wiener-index values. Table 5 lists the Wiener index $W(G)$ found for each molecular graph in the test set. For every graph, the values agreed exactly across all computation modes applicable to it (agreement wherever applicable); for C_1 and the cycles only the direct computation was available, and those values were checked against the closed forms below.

Table 5. Wiener index of the test set.

Family	Molecule	n	$W(G)$	Modes
Tree (reference)	Ten-vertex example	10	158	FW, LD, PP
Alkane	C_1 (methane)	1	0	FW
Alkane	C_2 (ethane)	2	1	FW, LD, PP
Alkane	C_3 (propane)	3	4	FW, LD, PP
Alkane	C_4 (n-butane)	4	10	FW, LD, PP
Alkane	C_5 (n-pentane)	5	20	FW, LD, PP
Alkane	C_6 (n-hexane)	6	35	FW, LD, PP
Alkane	C_7 (n-heptane)	7	56	FW, LD, PP
Alkane	C_8 (n-octane)	8	84	FW, LD, PP
Alkane	C_9 (n-nonane)	9	120	FW, LD, PP
Alkane	C_{10} (n-decane)	10	165	FW, LD, PP
Cycle	C_3	3	3	FW
Cycle	C_4	4	8	FW
Cycle	C_5	5	15	FW
Cycle	C_6 (benzene/cyclohexane)	6	27	FW
Cycle	C_7	7	42	FW
Cycle	C_8	8	64	FW
Dendrimer	$T_{2,3}$	10	117	FW, LD, PP
Dendrimer	$T_{3,3}$	22	909	FW, LD, PP

FW: Floyd-Warshall + sum; LD: leaf-deletion [2]; PP: pendant-path reduction (proposed). Methods not listed for a graph are not applicable to it.

The Wiener index of the n-alkane series grows as a smooth cubic, in agreement with the closed form $W(P_n) = n(n^2-1)/6$ that follows from the edge-decomposition of Abu-Affash et al. [1]. The cycle values match $W(C_n) = n^3/8$ for even n, which follows from the cut method of Klavžar and Romih [10] because even cycles are partial cubes, and $W(C_n) = n(n^2-1)/8$ for odd n. The dendrimer values $W(T_{2,3}) = 117$ and $W(T_{3,3}) = 909$ are verified independently in Section 6.5.

6.3. The ten-vertex example worked through. The ten-vertex tree G has vertex set $\{v_1, \dots, v_{10}\}$ and the nine edges $E(G) = \{v_1v_2,\ v_1v_3,\ v_1v_4,\ v_4v_5,\ v_5v_6,\ v_6v_7,\ v_7v_8,\ v_8v_9,\ v_9v_{10}\}$; vertex v_1 is a degree-three hub, and the chain $v_4v_5 \cdots v_{10}$ terminates at the leaf v_{10} (Figure 3a). The full 10×10 distance matrix (Figure 3b) was built by Floyd–Warshall. Its row sums, which are the vertex transmissions, are $30,38,38,26,24,24,26,30,36,44$ for $v_1, \dots, v_{10}$; their total is 316, so by (4) $W(G) = 316/2 = 158$. The same value follows from the edge decomposition (5): the nine edges, in the order listed, contribute $9,9,21,24,25,24,21,16,9$, again summing to 158. The cut removes the pendant path $u_1u_2u_3 = v_8v_9v_{10}$ ($k = 3$; only v_{10} is a leaf) with anchor $a = v_7$. The reduced tree T' on $v_1, \dots, v_7$ (written G' in Figure 3c) has transmissions $12,17,17,11,12,15,20$, with total 104, so $W(T') = 52$ and $Tr_{T'}(v_7) = 20$. Substituting $n = 10$ and $k = 3$ in (7) gives

$$W_{\text{path}} = W(P_3) + (n-k) \cdot \frac{k(k+1)}{2} + k \cdot \text{Tr}_{T'}(7) =$$

where $W(P_3) = 3(3^2-1)/6 = 4$ is the contribution of the pairs inside the removed path, $(n-k) \cdot k(k+1)/2 = 7 \cdot 6 = 42$ is the cross term, and $k \cdot Tr_{T'}(7) = 3 \cdot 20 = 60$, with $Tr_{T'}(7)$ the transmission of v_7 in T'. The sum $W(T') + W_{path} = 52 + 106 = 158$ recovers the Wiener index of the full tree exactly. The distance matrix dropped from 45 to 21 independent entries, a reduction of $24/45 \approx 53\%$. The edge list, both distance matrices and the MATLAB script that reproduces these numbers are provided in Supplementary Files S1 and S2.

6.4. Computational timings. Table 6 reports representative running times of the three computation modes. Steady-state times are the [median] of [N] repeated calls measured after a warm-up call, so that just-in-time (JIT) compilation and other first-call overheads are excluded from the comparison; first-call (cold-start) times, which are dominated by these overheads, are listed separately in the lower part of Table 6 and are not used in any comparison. In the steady state, all three procedures complete in well under one millisecond per graph at the molecular sizes considered. The Floyd–Warshall stage costs $O(n^3)$, the leaf-deletion stage runs in linear time [2], and the reduction stage adds an $O(n)$ chain-detection and anchor-transmission overhead before running a smaller Floyd–Warshall on the reduced graph.

Table 6. Representative running times (in milliseconds). Upper part: steady-state times; lower part: first-call times, shown separately and excluded from the comparison.

Molecule	n	FW + sum	Leaf-deletion	Pendant-path
n-octane (C_8)	8	0.04	0.02	0.15
n-decane (C_{10})	10	0.07	0.02	0.15
Dendrimer $T_{2,3}$	10	0.08	0.21	—
Dendrimer $T_{3,3}$	22	0.57	0.04	0.75
First-call (cold-start) times, excluded from the comparison				
Ten-vertex tree	10	14.0	39.6	104.7
Dendrimer $T_{2,3}$	10	—	—	6.58

Steady-state values: [median] of [N] calls after a warm-up call (MATLAB [release]; [processor, memory]). First-call values include JIT compilation and are reported only for completeness. —: no value in that regime.

For the graphs in Table 6, leaf-deletion [2] was faster than the Floyd–Warshall computation for n-octane, n-decane and $T_{3,3}$, but not for $T_{2,3}$. The pendant-path reduction was slower than the direct Floyd–Warshall computation for every graph measured, so no wall-clock speedup is claimed for it: at these sizes, locating the pendant chain and evaluating the anchor transmission cost more than the smaller matrix saves. The reduction is therefore presented as an analytic simplification rather than as a wall-clock accelerator. Figure 5 shows the steady-state times.

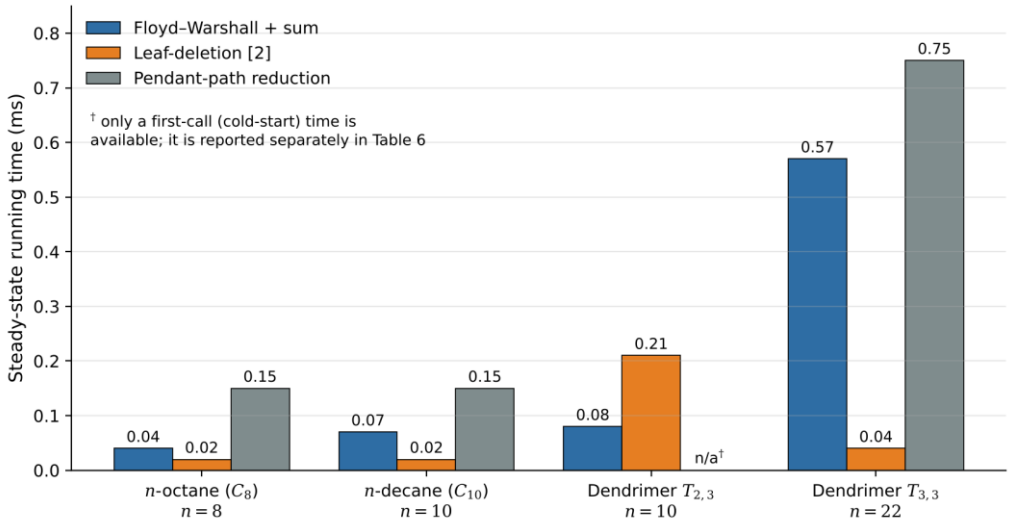


Figure 5. Steady-state Wiener-index computation times (ms) for the graphs in Table 6; first-call (JIT-affected) times are excluded.

6.5. Validation against published and independent results. The Wiener-index values of the n-alkane chain reproduce the closed form $W(P_n) = n(n^2-1)/6$, which follows from the edge decomposition (5) recorded by Abu-Affash et al. [1] and is implicit in the analysis of Damnjanović et al. [5]. The cycle C_6 yields $W = 27$, in agreement with $W(C_6) = 6^3/8$ from the cut method of Klavžar and Romih [10]. For the dendrimers, all values in this paper count each unordered pair of vertices once, as in (3), and two independent checks were made. First, by (5): in $T_{2,3}$ each of the three root edges separates 3 from 7 vertices and each of the six leaf edges separates 1 from 9, giving $3 \cdot 21 + 6 \cdot 9 = 117$; in $T_{3,3}$ the three edge classes give $3 \cdot (7 \cdot 15) + 6 \cdot (3 \cdot 19) + 12 \cdot (1 \cdot 21) = 315 + 342 + 252 = 909$. Second, through the Hosoya polynomial (6): $T_{2,3}$ has 9,12,12,12 unordered pairs at distances 1,2,3,4, so $W = H'(T_{2,3}, 1) = 9 + 24 + 36 + 48 = 117$, and $T_{3,3}$ has 21,30,36,48,48,48 pairs at distances $1, \ldots, 6$, so $W = 21 + 60 + 108 + 192 + 240 + 288 = 909$. In a tree each unordered pair of vertices is joined by exactly one path, so these pair counts are the numbers of paths of each length that Tabassum et al. [16] enumerate for dendrimers. If distances are instead summed over ordered pairs (u, v), that is, over all entries of $D(G)$ rather than its upper triangle, every pair is counted twice and the totals double (234 for $T_{2,3}$ and 1818 for $T_{3,3}$); the values reported here use the unordered convention throughout.

7. Discussion

This section interprets the numerical results of Section 6 in the light of the works surveyed in Section 5: the cost-benefit profile of the pendant-path cut, its relation to the linear-time method of Bi et al. [2] and the cut method of Klavžar and Romih [10], and its limitations on structures without a long pendant chain.

7.1. Cost-benefit profile of the reduction. The reduction transforms the $n \times n$ distance matrix of a chemical tree into an $(n-k) \times (n-k)$ distance matrix and recovers the original Wiener index through the closed-form correction (7). The number of independent distance entries drops from $n(n-1)/2$ to $(n-k)(n-k-1)/2$, a saving of $[n(n-1) - (n-k)(n-k-1)]/2$ entries. For the ten-vertex

tree with $k = 3$, the saving is $45 - 21 = 24$ entries out of 45, about 53%. The saving grows with k: for an alkane P_n with $k = n - 1$, the reduced tree is a single vertex, no distance entries remain, and (7) with $Tr_{T'}(a) = 0$ gives $W(P_{n-1}) + n(n-1)/2 = n(n^2 - 1)/6$ directly.

At the molecular sizes studied, the measured steady-state time of the cut was higher than that of the direct Floyd–Warshall computation (Table 6), because locating a suitable pendant chain and computing the anchor transmission cost more than the operations saved for $n \leq 22$. In terms of operation counts, the Floyd–Warshall stage on the reduced tree performs $(n-k)^3$ instead of n^3 relaxation steps, so a wall-clock advantage could appear only for larger trees with long pendant chains; this was not tested here, and no speedup is claimed. The use of the cut at these sizes is thus mainly analytic: the distance matrix is replaced by a smaller matrix plus a single closed-form expression.

7.2. Relation to the leaf-deletion algorithm and cut method. The leaf-deletion procedure of Bi et al. [2] corresponds to the case $k = 1$ of the pendant-path reduction, iterated until the graph reduces to a single vertex. Taking $k > 1$ means that a pendant chain is detected once rather than vertex by vertex; this is a statement about operation counts, not a measured speedup (Section 6.4). For the ten-vertex tree with $k = 3$, the chain $v_{10}v_9v_8$ is detected in a single pass, the contribution $4 + 42 + 60 = 106$ is computed in closed form, and the remaining value $W(T') = 52$ is the ordinary Wiener index of the seven-vertex tree.

The leaf-deletion procedure instead removes v_{10}, v_9 and v_8 in three passes, accumulating the edge contributions $1 \cdot 9 = 9$, $2 \cdot 8 = 16$ and $3 \cdot 7 = 21$ (total 46); it then continues on the seven-vertex tree in which the anchor v_7 carries the weight $count[v_7] = 4$, so that the remaining edges contribute 112 rather than $W(T') = 52$. Both routes give 158: the closed-form correction 106 equals the 46 accumulated on the chain edges plus $60 = k \cdot Tr_{T'}(v_7)$, which leaf-deletion accounts for through the weight on the anchor. The same observation applies to the cut method of Klavžar and Romih [10]: for a pendant chain of k vertices, the contribution of the chain edges is the sum that appears in the leaf-deletion analysis, and (7) closes this into a single formula that makes explicit the role of the anchor transmission left implicit in the iterative formulations.

7.3. Limitations and applicability. The reduction operates on trees that contain a pendant path of the desired length. Cyclic structures, including C_6, C_7, and C_8, contain no pendant vertex and therefore admit neither the leaf-deletion procedure nor the proposed reduction; for these graphs the Floyd–Warshall computation is the available option, and it yields the textbook value $W(C_6) = 27$. Klavžar and Romih [10] address the cyclic case through their cut method, whose Θ-classes can include non-pendant edges. Highly branched trees such as the dendrimer $T_{r,\delta}$ [16] give a different limitation: every non-leaf vertex has degree $\delta \geq 3$, so the longest available pendant path has $k = 1$ vertex, and the cut gives only a small saving, equivalent to one iteration of leaf-deletion.

The cut is thus most useful on chemical trees with at least one long pendant chain, such as the n-alkane skeleton, or on trees obtained by attaching short alkyl substituents to alkanes. A second limitation is the assumption of a simple unweighted, hydrogen-suppressed graph; the extension to the weighted Wiener index $W_a(G^D)$ of Brezovnik et al. [4] requires the closed-form correction to use the weighted transmission and is left for future work. A third limitation concerns the position of the pendant chain: removing multiple long branches simultaneously, each evaluated against its own anchor, is consistent with the cut method of [10] but lies beyond the present scope.

7.4. Quality assessment of the surveyed references. Each of the twenty references was evaluated on five criteria: (i) explicit definition of the Wiener index or a close variant; (ii) a clear methodology section; (iii) explicit statement of the main result with proof or numerical evidence; (iv) declaration of limitations or future work; and (v) open access. Table 7 summarises the outcome: all twenty references satisfy at least four of the five criteria, the only frequent gap being an explicit declaration of limitations or future work.

Table 7. Quality assessment of the twenty surveyed references against five SLR criteria.

Ref	(i) W def.	(ii) Method	(iii) Result	(iv) Limits/Future	(v) Open	Score
[5]	•	•	•	•	•	5/5
[3]	•	•	•	•	•	5/5
[13]	•	•	•	•	•	5/5
[10]	•	•	•	•	•	5/5
[1]	•	•	•	•	•	5/5
[2]	•	•	•		•	4/5
[7]	•	•	•	•	•	5/5
[6]	•	•	•	•	•	5/5
[9]	•	•	•		•	4/5
[17]	•	•	•	•	•	5/5
[16]	•	•	•		•	4/5
[4]	•	•	•	•	•	5/5
[8]	•	•	•	•	•	5/5
[19]	•	•	•	•	•	5/5
[18]	•	•	•	•	•	5/5
[20]	•	•	•	•	•	5/5
[15]	•	•	•	•	•	5/5
[14]	•	•	•	•	•	5/5
[11]	•	•	•	•	•	5/5
[12]	•	•	•	•	•	5/5
Total	**20**	**20**	**20**	**17**	**20**	**97/100**

7.5. Recommendation framework for practitioners. The choice of method depends on the form of the graph. (a) For a linear alkane series P_n, or any tree whose longest pendant path has close to n vertices, the pendant-path cut is the most informative method analytically, reducing the $n \times n$ matrix to a single closed-form expression. (b) For an arbitrary tree, the linear-time leaf-deletion method of Bi et al. [2] is recommended at moderate-to-large sizes and remains correct on unicyclic graphs. (c) For highly branched dendrimers $T_{r,\delta}$ [16], the path counts of Tabassum et al. or the edge decomposition (5) give the Wiener index directly. (d) For benzenoid hydrocarbons and other partial-cube graphs, the cut method of Klavžar and Romih [10] is the standard. (e) For weighted molecular graphs with multiple bonds, the Floyd–Warshall + sum method of Brezovnik et al. [4] is required. (f) For very large fullerene oligomers, the topological-efficiency approach of Sabirov et al. [14] scales well.

8. Conclusion

This paper has surveyed twenty recent works (2021–2026) on the Wiener index of chemical graphs, formalised the pendant-path reduction, implemented it in MATLAB, and applied it to nineteen molecular graphs spanning trees, n-alkanes, cycles, and dendrimers. The reduction reproduces the Wiener index of the original graph in every case to which it applies, with the contribution of the removed pendant path captured in closed form by (7). The numerical values match the closed forms $W(P_n) = n(n^2-1)/6$ for paths [1] and $W(C_n) = n^3/8$ for even cycles, consistent with the cut method of Klavžar and Romih [10], and the dendrimer values $W(T_{2,3}) = 117$ and $W(T_{3,3}) = 909$ were confirmed

independently through the edge decomposition and the path counts underlying Tabassum et al. [16].

The proposed reduction is best understood as the multi-vertex generalisation of the linear-time leaf-deletion algorithm of Bi et al. [2] and as a closed-form simplification of the cut method of Klavžar and Romih [10] for pendant paths. Taking $k > 1$ processes a pendant chain in one step instead of k; at the molecular sizes studied, however, no wall-clock speedup was observed, and the benefit is the analytic simplification of the distance matrix from $n \times n$ to $(n-k) \times (n-k)$ in every applicable case. Because the graphs are hydrogen-suppressed connectivity models, the results concern shortest-path distance matrices and topological descriptors, not chemical reaction pathways, and equal topology does not imply equal chemical properties. The extension of the reduction to edge-weighted molecular graphs [4], the simultaneous removal of multiple pendant chains in the spirit of [10], the extension to unicyclic and bicyclic graphs [2, 11], and the application to larger fullerene oligomers [14] are natural directions for future work.

Acknowledgements

The authors thank the open-access publication ecosystem of arXiv.org and MDPI, which made the twenty reference papers freely available, and acknowledge the developers of MATLAB and of the NetworkX graph-theory library, used in the implementation and figure-generation stages of this work.

Author Contributions

Z.M. Abed conceived the study, derived the closed-form correction of Section 4.3, wrote the MATLAB scripts, and ran the numerical experiments. W.R. Dawood conducted the literature search and selection, generated the figures, and contributed to the comparative analysis. Both authors wrote and reviewed the manuscript, and have read and agreed to the published version of the manuscript.

Conflict of Interest

The authors declare no conflict of interest.

Funding

The authors declare that no funds, grants, or other support were received during the preparation of this manuscript.

Data Availability

The data and code supporting this study are provided as supplementary material with this article. Supplementary File S1 contains the MATLAB source code (graph construction, Floyd–Warshall distance matrices, direct summation, leaf-deletion, pendant-path reduction, and the timing script). Supplementary File S2 contains the edge lists of all nineteen test graphs, the distance matrices of the ten-vertex tree before and after the reduction, the computed Wiener-index values with the modes applied, and the distance distributions of the two dendrimers. Supplementary File S3 contains the catalogue of the twenty surveyed references with their DOIs or URLs, axis coding (Table 4) and quality scores (Table 7). The surveyed references are open access and can be retrieved from the links in the reference list. The screening log of the 44 candidate papers and the per-paper structured summaries are available from the corresponding author on reasonable request. No proprietary or restricted data were used in this study.

References

[1] A.K. Abu-Affash, P. Carmi, O. Luwisch and J.S.B. Mitchell, *Geometric spanning trees minimizing the Wiener index*, arXiv:2303.01096, 2023. https://arxiv.org/abs/2303.01096

[2] B. Bi, M.K. Jamil, K.M. Fahd, T.-L. Sun, I. Ahmad and L. Ding, *Algorithms for computing Wiener indices of acyclic and unicyclic graphs*, Complexity **2021**, art. 6663306, 2021. https://doi.org/10.1155/2021/6663306

[3] B. Borovićanin, D. Božović, E. Glogić, D. Mesarič Štesl, S. Špacapan and E. Zogić, *New results on the Wiener index of trees with a given diameter*, arXiv:2507.17885, 2025. https://arxiv.org/abs/2507.17885

[4] S. Brezovnik, N. Tratnik and P. Žigert Pleteršek, *Weighted Wiener indices of molecular graphs with application to alkenes and alkadienes*,

Mathematics **9** (2), art. 153, 2021. https://doi.org/10.3390/math9020153

[5] I. Damnjanović, A. Xu and K. Xu, *On the transmission irregular trees with the maximum Wiener index*, J. Comb. Optim. **51**, art. 12, 2026; preprint arXiv:2512.13585. https://arxiv.org/abs/2512.13585

[6] P. Dankelmann, *Distance sequences to bound the Harary index and other Wiener-type indices of a graph*, arXiv:2411.13439, 2024. https://arxiv.org/abs/2411.13439

[7] H. Darabi, Y. Alizadeh, S. Klavžar and K.C. Das, *On the relation between Wiener index and eccentricity of a graph*, arXiv:2103.02307, 2021. https://arxiv.org/abs/2103.02307

[8] H. Ibrahim, R. Sharafdini, T. Réti and A. Akwu, *Wiener–Hosoya matrix of connected graphs*, Mathematics **9** (4), art. 359, 2021. https://doi.org/10.3390/math9040359

[9] S. Khan and S. Pirzada, *On distance Laplacian spread and Wiener index of a graph*, arXiv:2210.10579, 2022. https://arxiv.org/abs/2210.10579

[10] S. Klavžar and G.D. Romih, *The cut method on hypergraphs for the Wiener index*, J. Math. Chem. **61**, 1592–1603, 2023. https://doi.org/10.1007/s10910-023-01478-4

[11] D. Li and S. Zhou, *On distance Laplacian energy of unicyclic and bicyclic graphs*, Axioms **14** (11), art. 825, 2025. https://doi.org/10.3390/axioms14110825

[12] Y. Mei and H. Miao, *The vertex Gutman index and Gutman index of the union of two cycles*, Axioms **13** (4), art. 269, 2024. https://doi.org/10.3390/axioms13040269

[13] A.N. Rabenantoandro, *Peripheral hyper-Wiener index of a graph*, arXiv:2512.13468, 2025. https://arxiv.org/abs/2512.13468

[14] D.Sh. Sabirov, O. Ori, A.A. Tukhbatullina and I.S. Shepelevich, *Covalently bonded fullerene nano-aggregates* $(C_{60})_n$*: digitalizing their energy–topology–symmetry*, Symmetry **13** (10), art. 1899, 2021. https://doi.org/10.3390/sym13101899

[15] U. Sheikh, S. Rashid, C. Ozel and R. Pincak, *On Hosoya polynomial and subsequent indices of* $C_4C_8(R)$ *and* $C_4C_8(S)$ *nanosheets*, Symmetry **14** (7), art. 1349, 2022. https://doi.org/10.3390/sym14071349

[16] H. Tabassum, S.A.U.H. Bokhary, T. Jiarasuksakun and P. Kaemawichanurat, *Counting the numbers of paths of all lengths in dendrimers and its applications*, arXiv:2201.01009, 2022. https://arxiv.org/abs/2201.01009

[17] S. Vaidya and A. Li, *Hosoya polynomials of Mycielskian graphs*, arXiv:2503.03055, 2025. https://arxiv.org/abs/2503.03055

[18] C. Xu and M. Liu, *The Steiner* k*-Wiener index of cacti*, Symmetry **17** (9), art. 1371, 2025. https://doi.org/10.3390/sym17091371

[19] J. Zeng, H. Liu and L. You, *Extremal results on ℓ-connected graphs or pancyclic graphs based on Wiener-type indices*, Mathematics **13** (1), art. 10, 2025. https://doi.org/10.3390/math13010010

[20] D. Zhao, Y. Zhao, Z. Wang, X. Li and K. Zhou, *Kirchhoff index and degree Kirchhoff index of tetrahedrane-derived compounds*, Symmetry **15** (5), art. 1122, 2023. https://doi.org/10.3390/sym15051122